

## Electronic Supplementary Information

Exploring Cyclohexane/Piperazine-urea Motifs for Spherical Halides (X= Cl<sup>-</sup> / Br<sup>-</sup>) Recognition: Effect on Anion Coordination, Photoluminescence, and Morphological Tunability

Megha Basak, Aresh Das, Gopal Das\*

Department of Chemistry, Indian Institute of Technology Guwahati, Assam 781039, India

gdas@iitga.ac.in

## Characterisation of L<sub>1</sub>

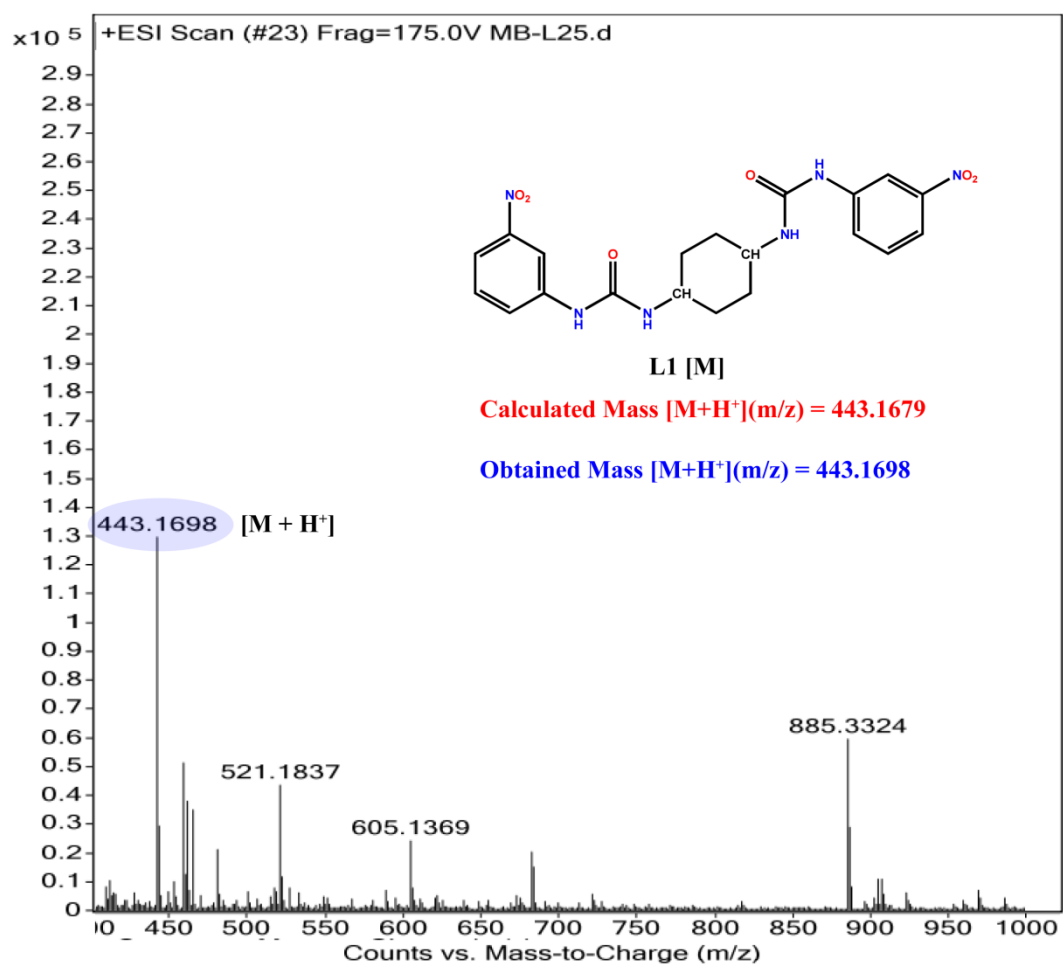


**Figure S1:** HRMS spectra of L<sub>1</sub> in 1:1 water-acetonitrile in positive ionization mode.

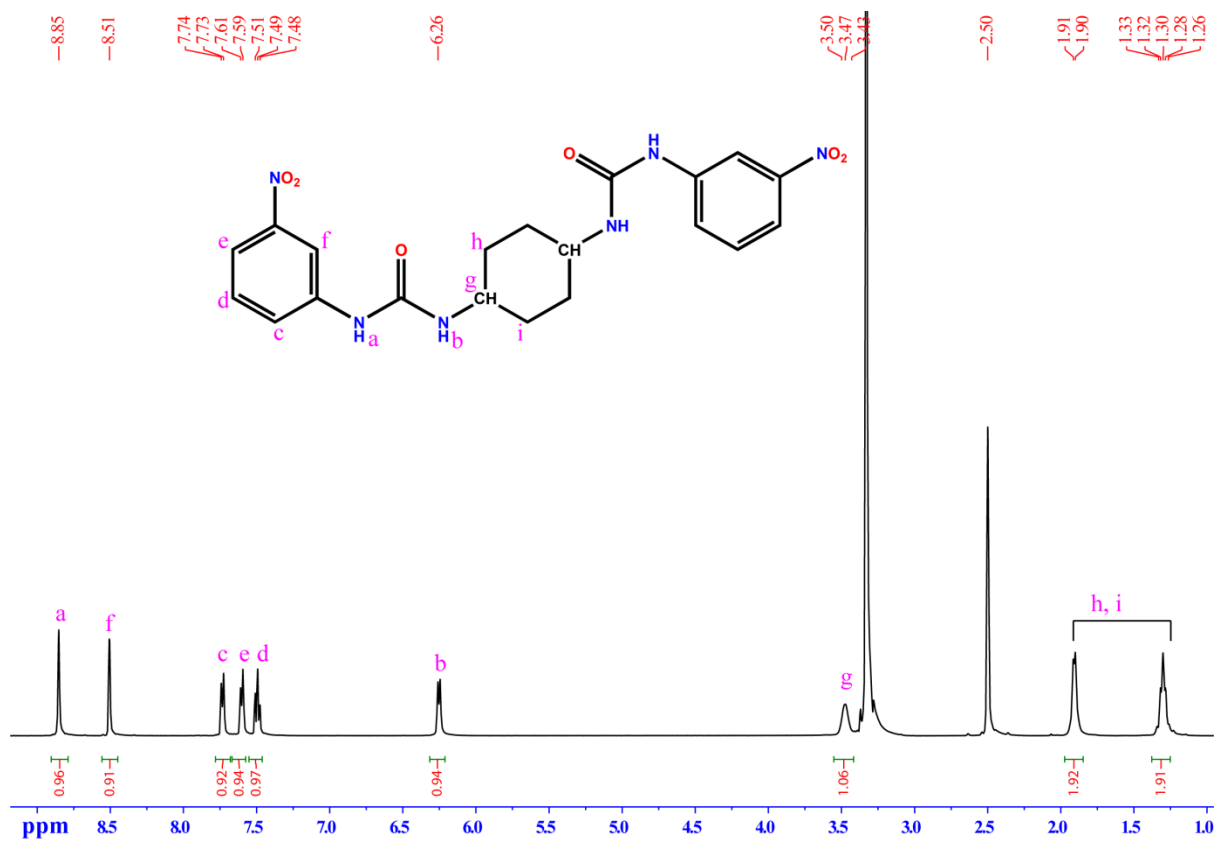


**Figure S2:** <sup>1</sup>H NMR spectra of **L1** in DMSO-d<sub>6</sub> at room temperature.

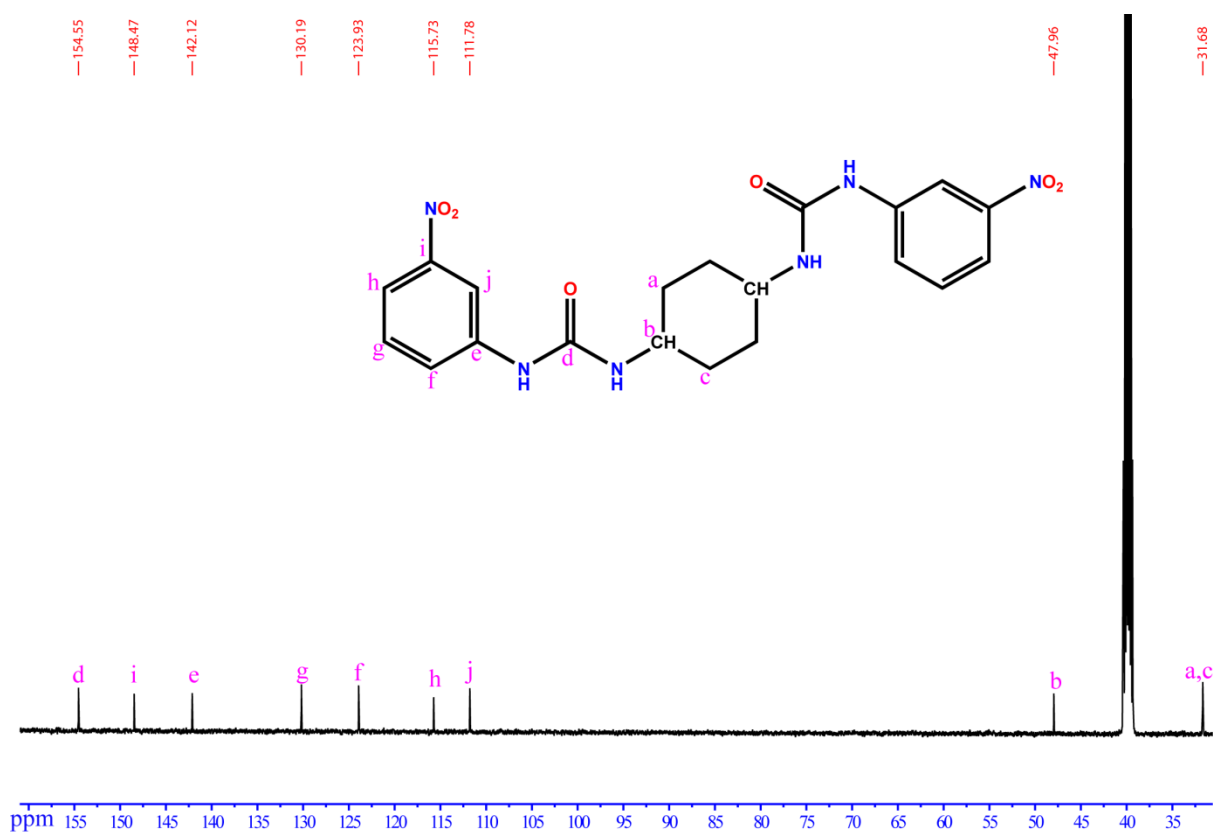


**Figure S3:**  $^{13}\text{C}$  NMR of  $\text{L}_1$  in  $\text{DMSO-d}_6$  at room temperature.

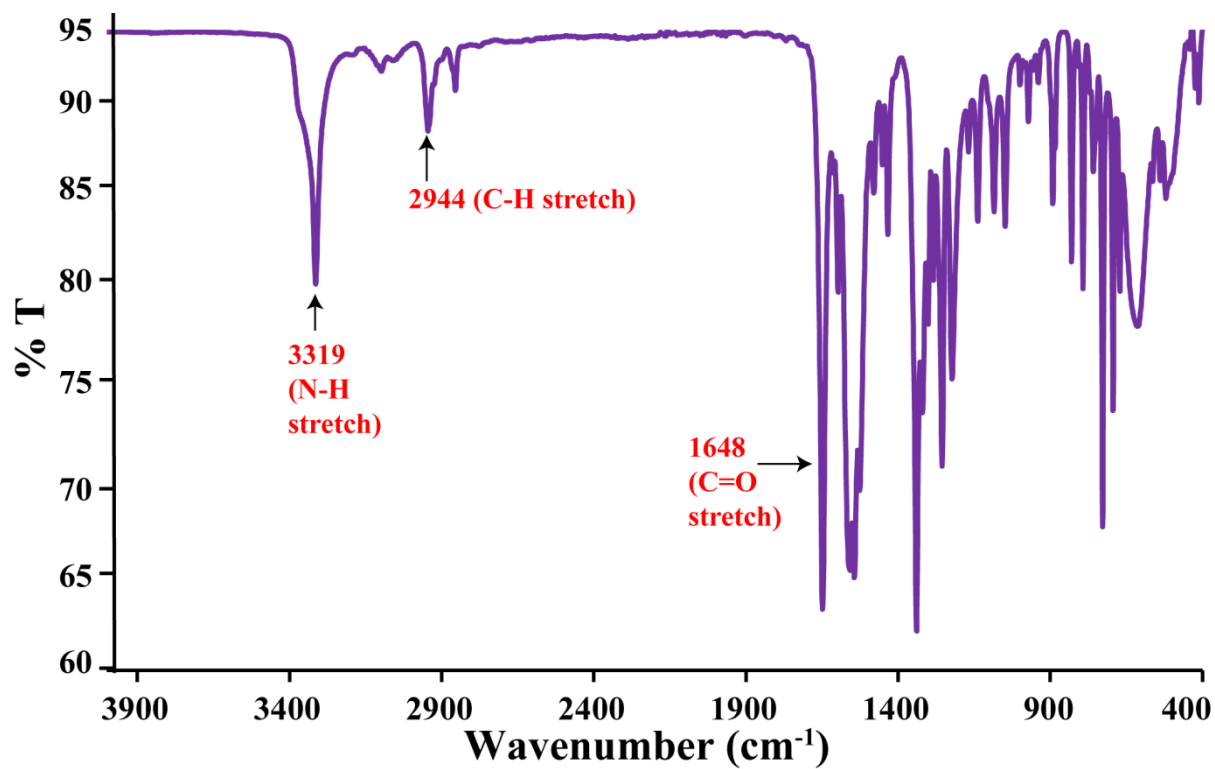


**Figure S4:** FTIR spectrum of L<sub>1</sub> recorded in KBr pellet at room temperature.

#### Characterisation of L<sub>2</sub>

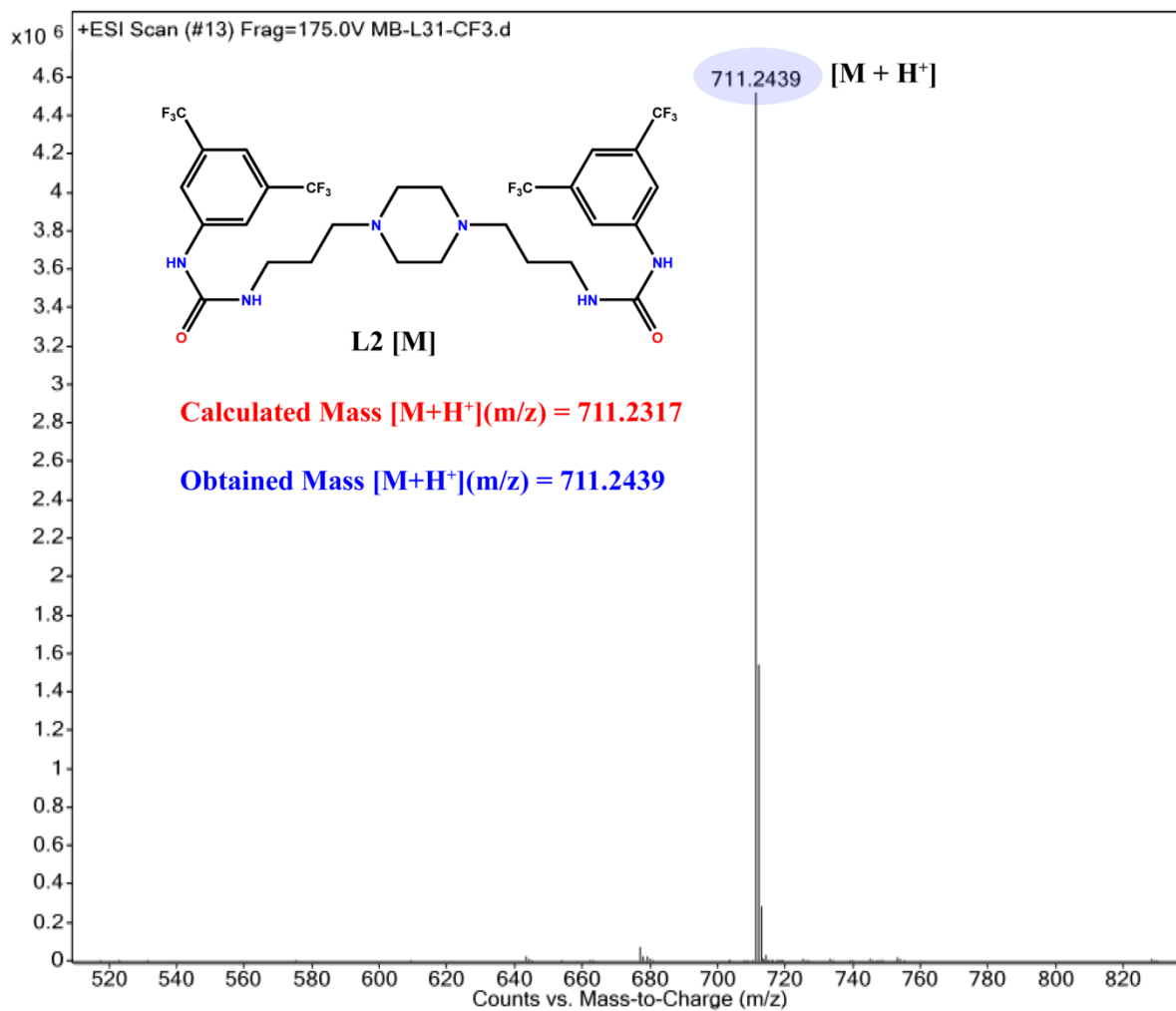


**Figure S5:** HRMS spectra of **L<sub>2</sub>** in 1:1 water-acetonitrile in positive ionization mode.



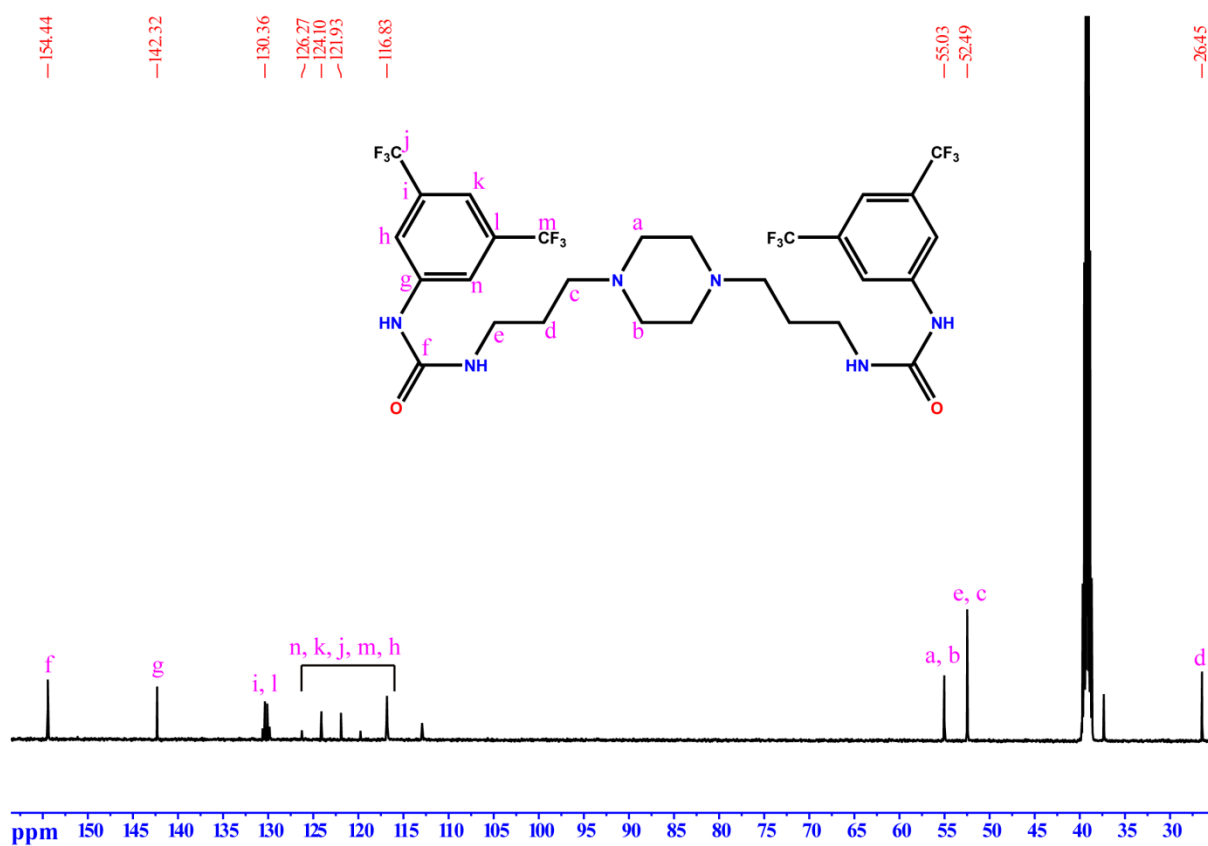


**Figure S7:**  $^{13}C$  NMR of  $L_2$  in  $DMSO-d_6$  at room temperature.

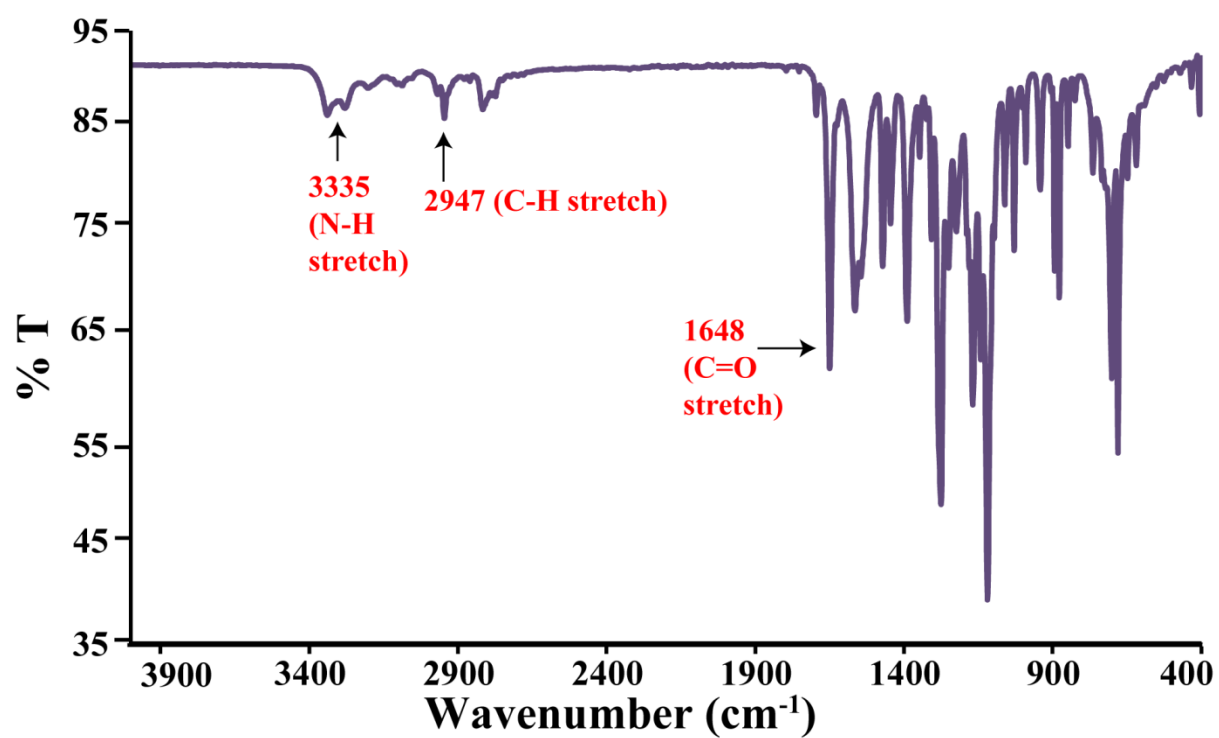


**Figure S8:** FTIR spectrum of L<sub>2</sub> recorded in KBr pellet at room temperature.

### Characterisation of complex 1a

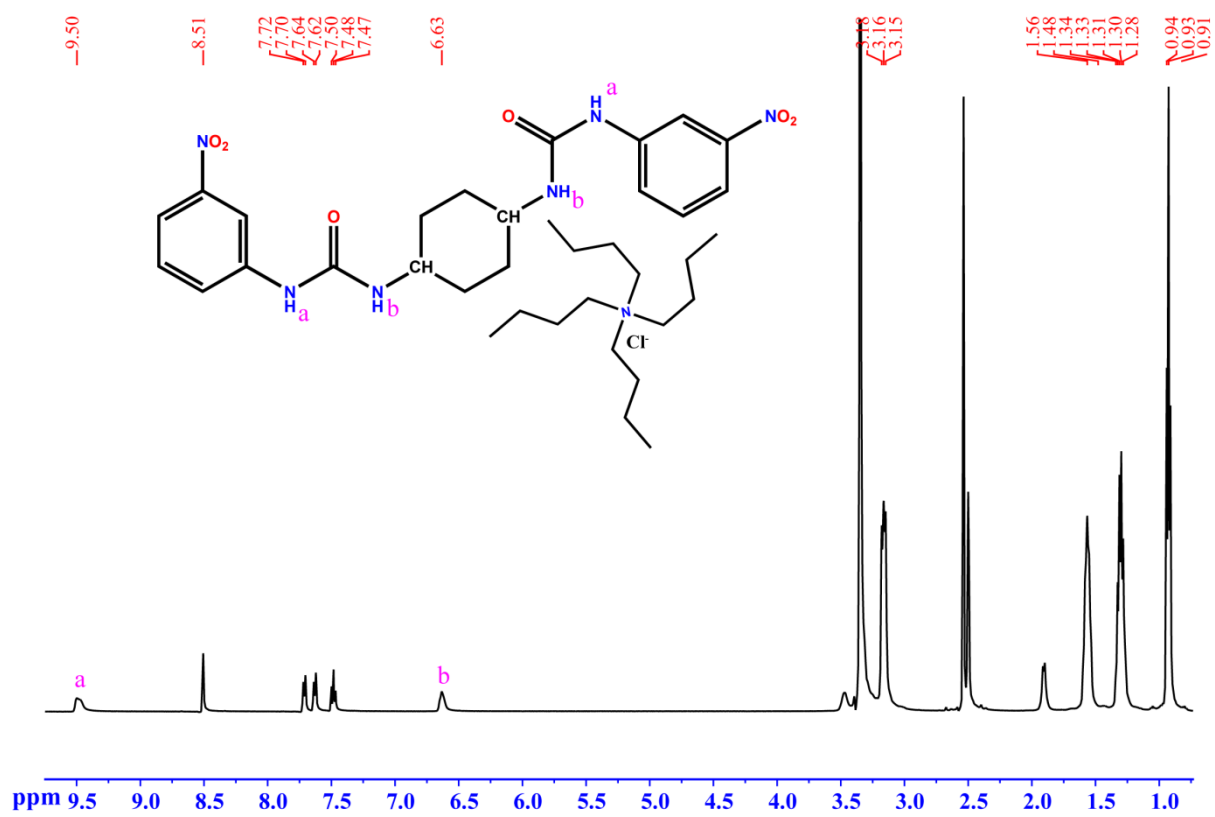


**Figure S9:**  $^1H$  NMR spectra of chloride complex of  $L_1(1a)$  in  $DMSO-d_6$  at room temperature.

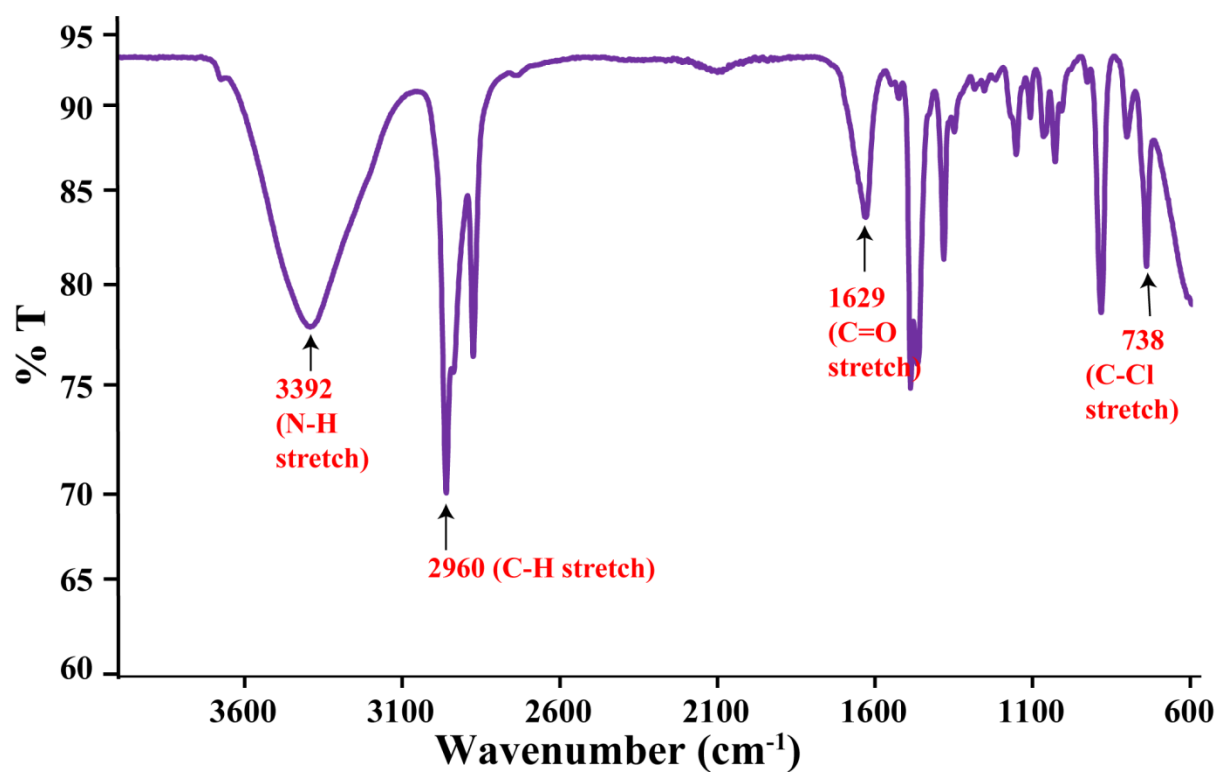


**Figure S10:** FTIR spectrum of chloride complex of  $L_1(1a)$  recorded in KBr pellet at room temperature.

#### Characterisation of complex 1b

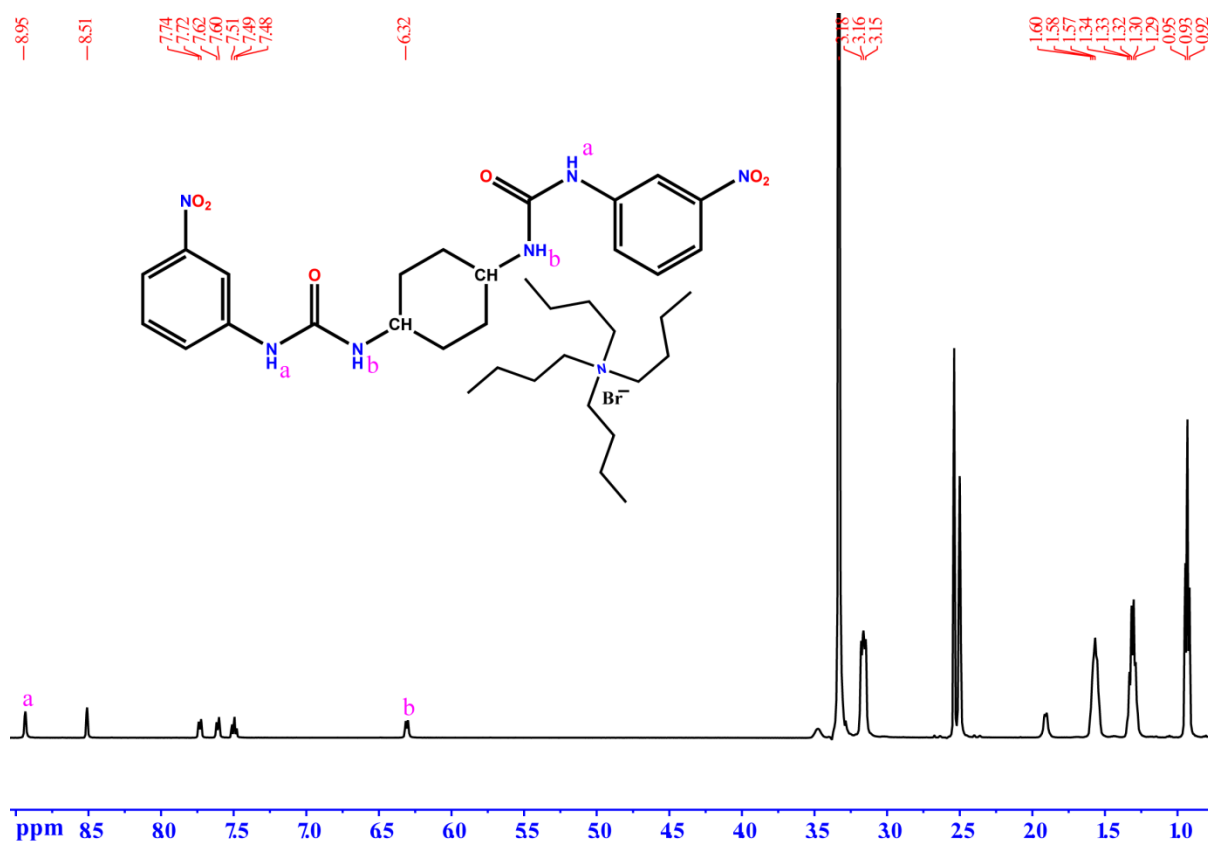


**Figure S11:**  $^1H$  NMR spectra of bromide complex of  $L_1(1b)$  in DMSO- $d_6$  at room temperature.

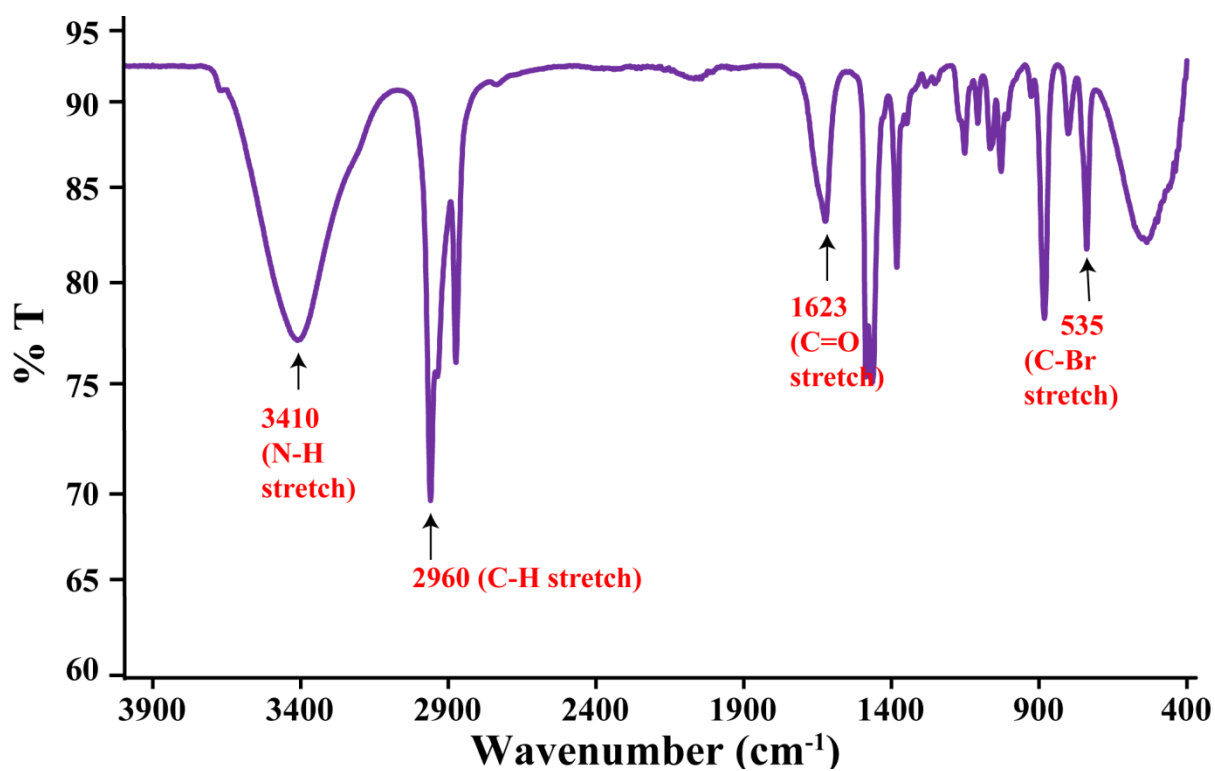


**Figure S12:** FTIR spectrum of bromide complex of  $L_1$ (**1b**) recorded in KBr pellet at room temperature.

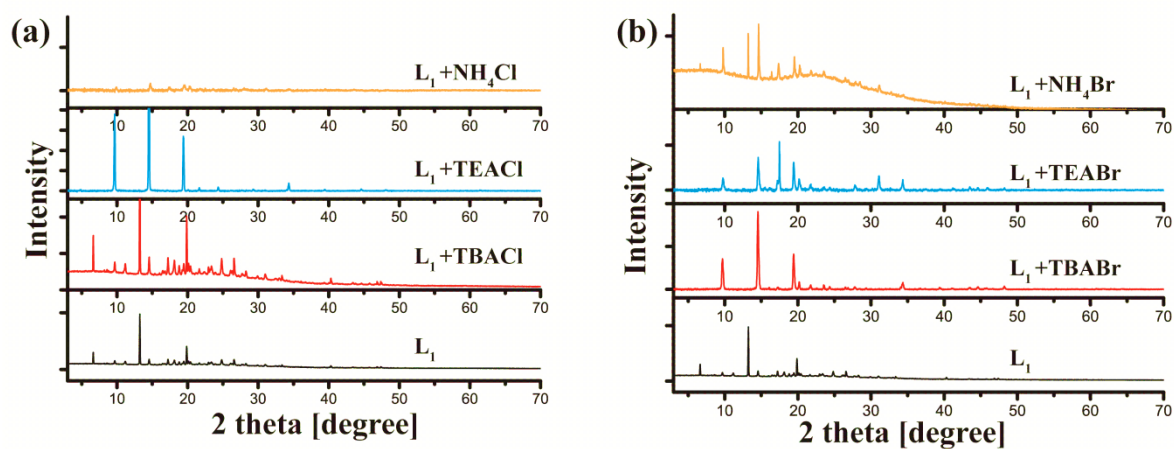


**Figure S13:** Comparative PXRD analysis of  $L_1$  varying the chain length of halogen salts (a). in presence of TBACl, TEACl and  $NH_4Cl$ . (b) in presence of TBABr, TEABr and  $NH_4Br$ .

## Characterisation of complex 2a

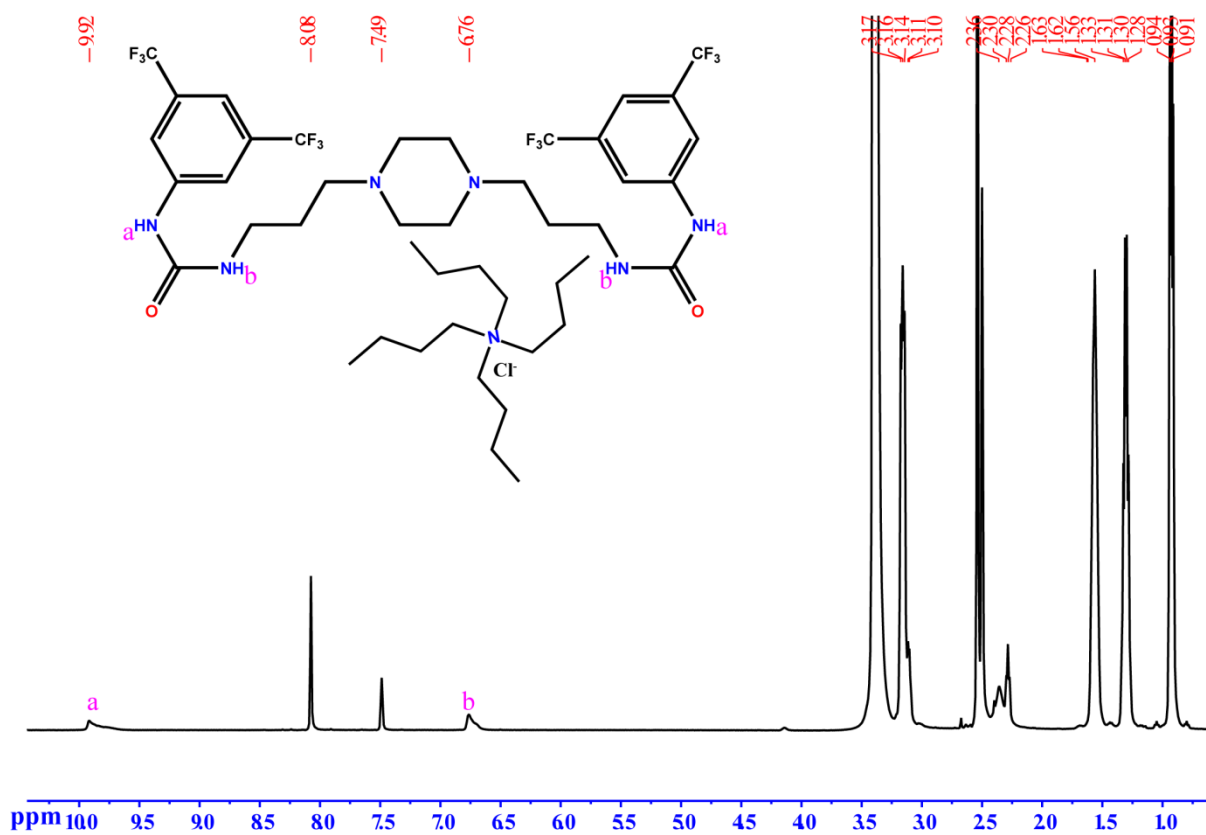


**Figure S14:**  $^1H$  NMR spectra of chloride complex of  $L_2(2a)$  in  $DMSO-d_6$  at room temperature.

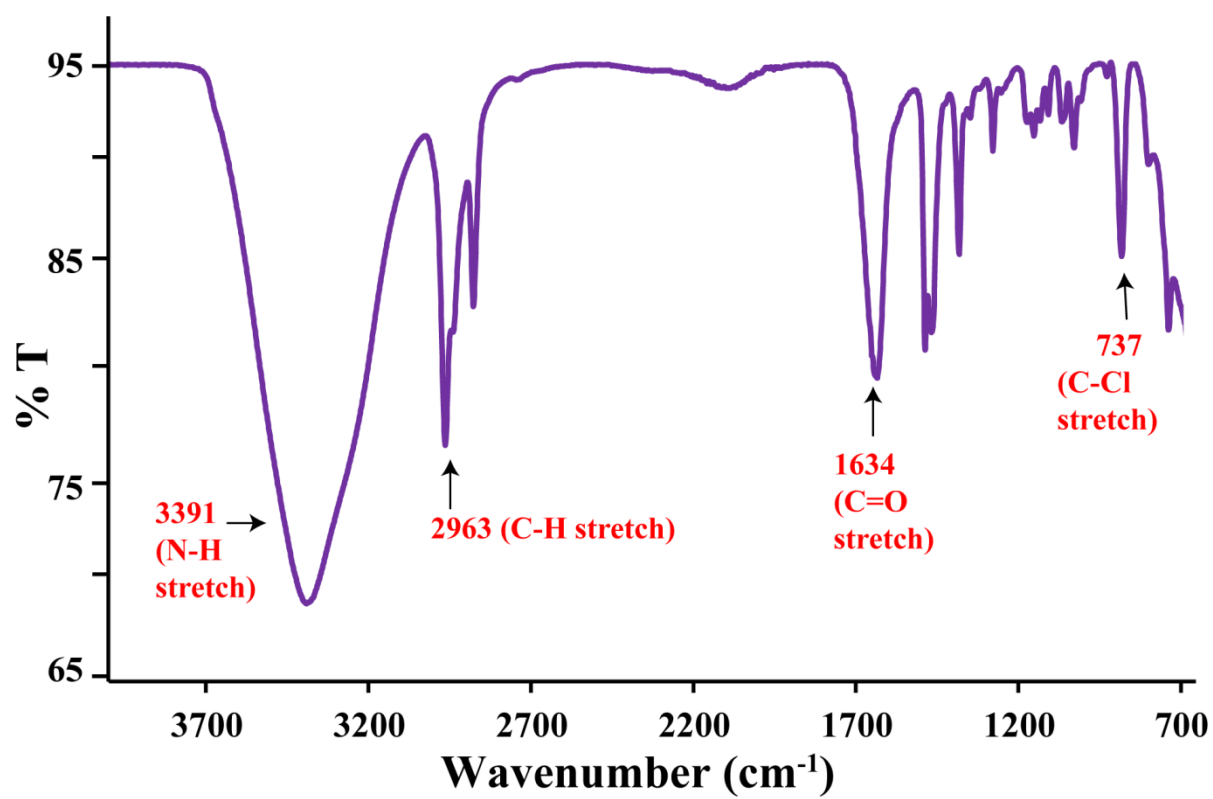


**Figure S15:** FTIR spectrum of chloride complex of  $L_2(2a)$  recorded in KBr pellet at room temperature.

## Characterisation of complex 2b

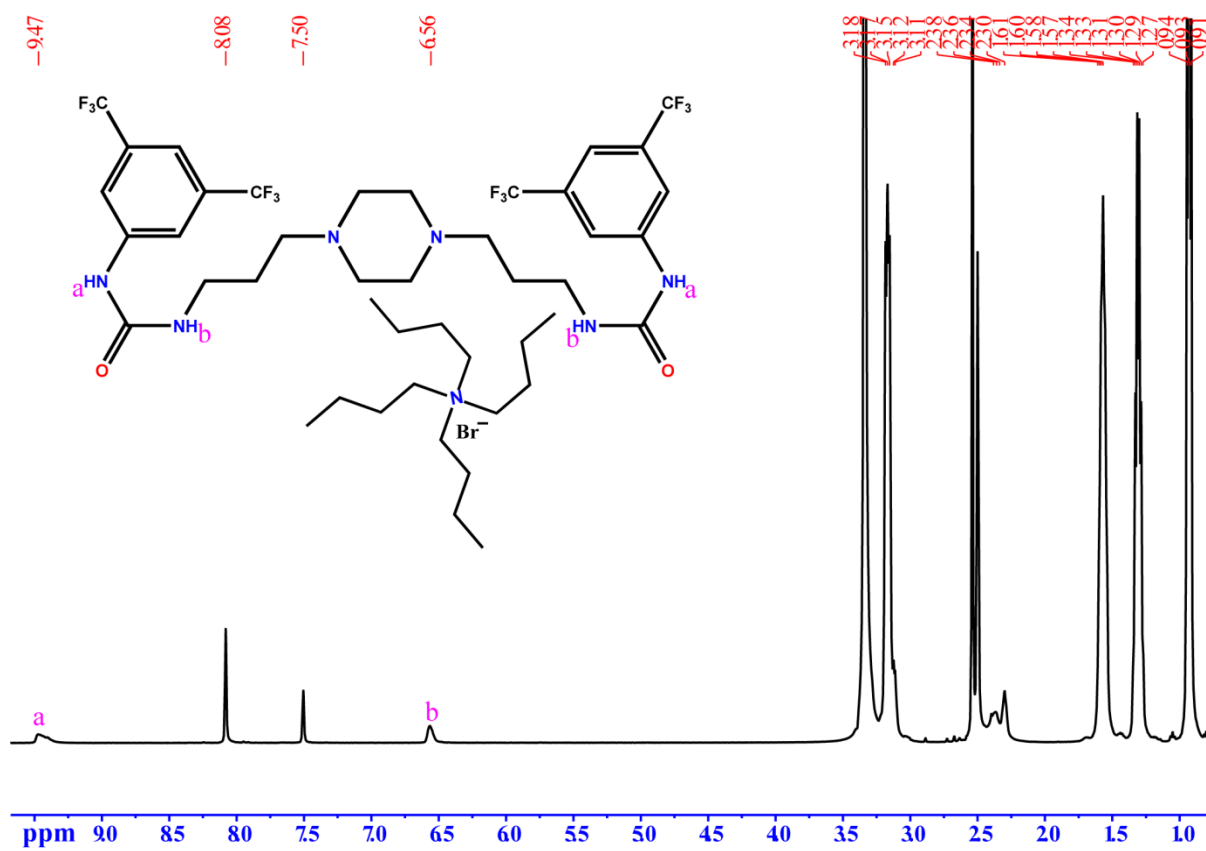


**Figure S16:**  $^1H$  NMR spectra of bromide complex of  $L_2(2b)$  in DMSO- $d_6$  at room temperature.

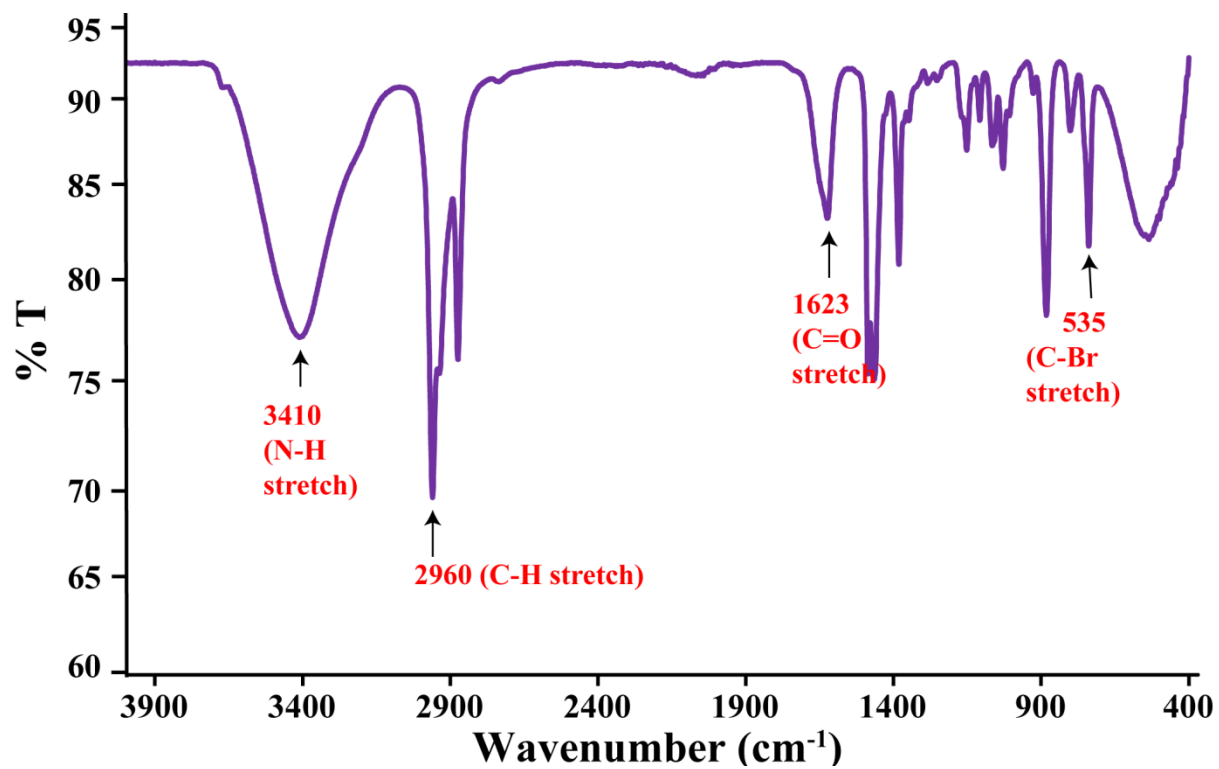


**Figure S17:** FTIR spectrum of bromide complex of  $L_2(2b)$  recorded in KBr pellet at room temperature.

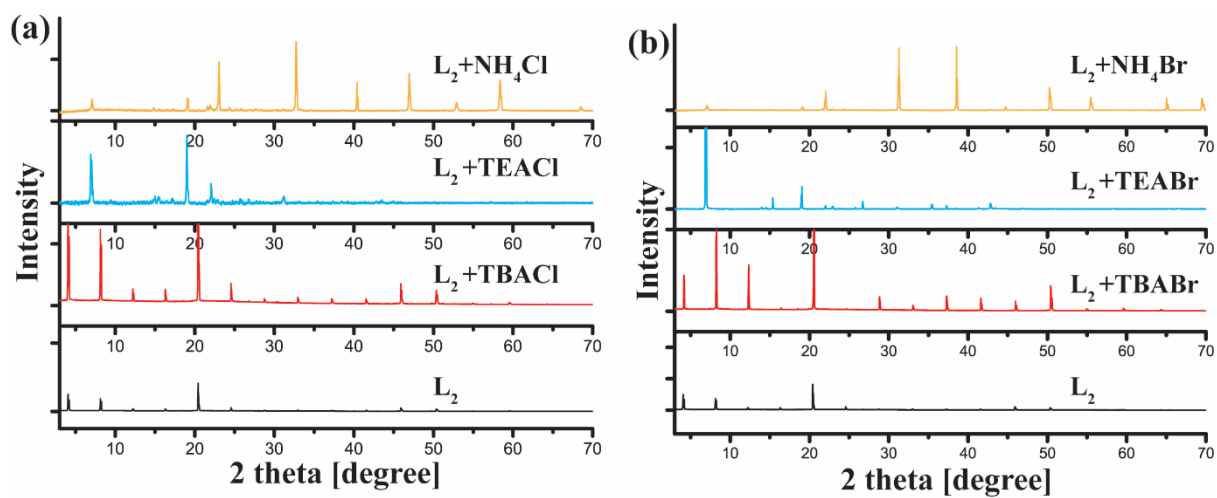


**Figure S18:** Comparative PXRD analysis of  $L_2$  varying the chain length of halogen salts (a) in presence of TBACl, TEACl and  $NH_4Cl$ . (b) in presence of TBABr, TEABr and  $NH_4Br$ .

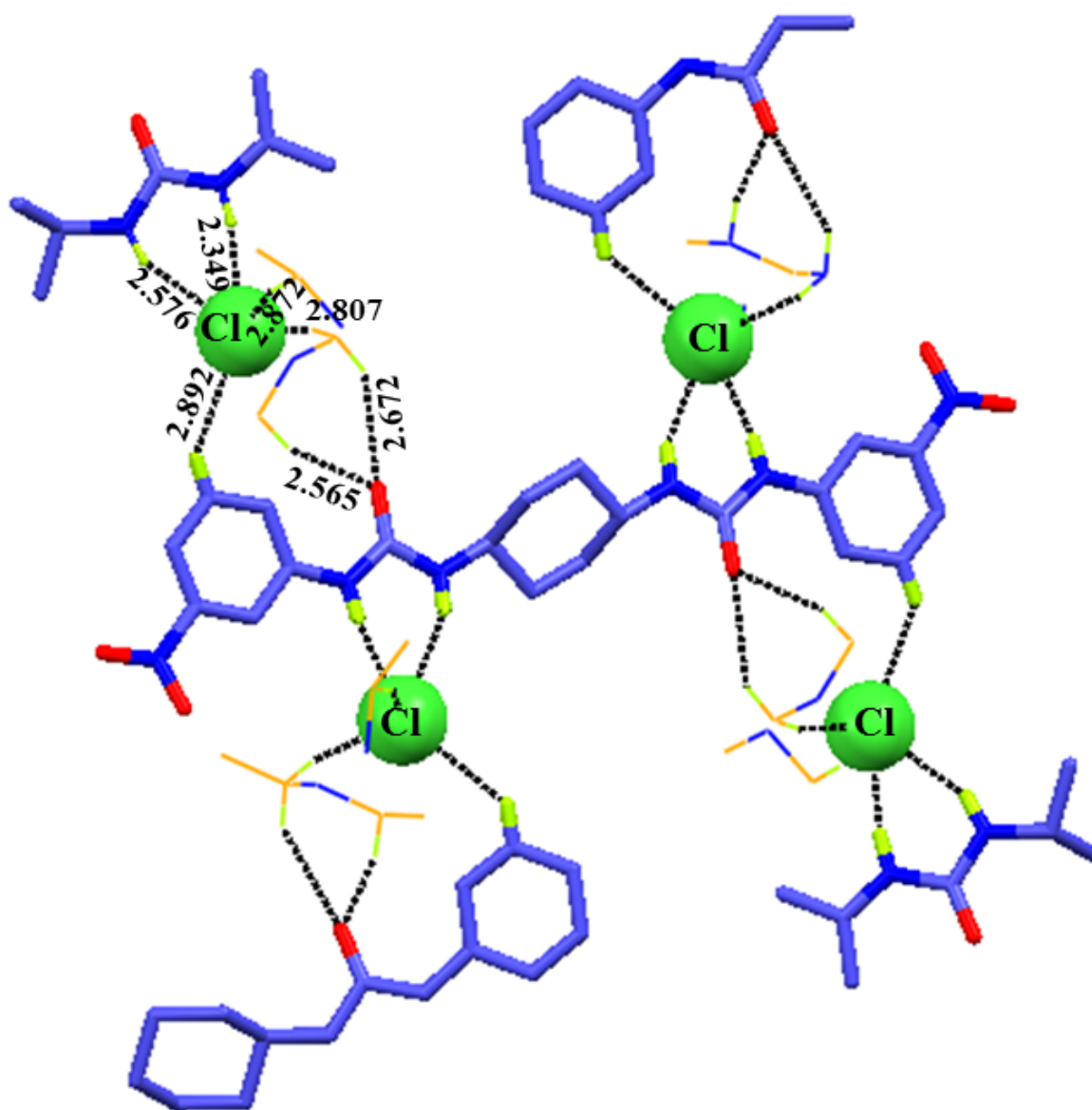


**Figure S19:** X-ray structure analysis of complex **1a** showing coordination environment of anion as well as extra stabilization through C-H<sub>aliphatic</sub>...O<sub>urea</sub> interaction with proper bond distances in Angstrom.

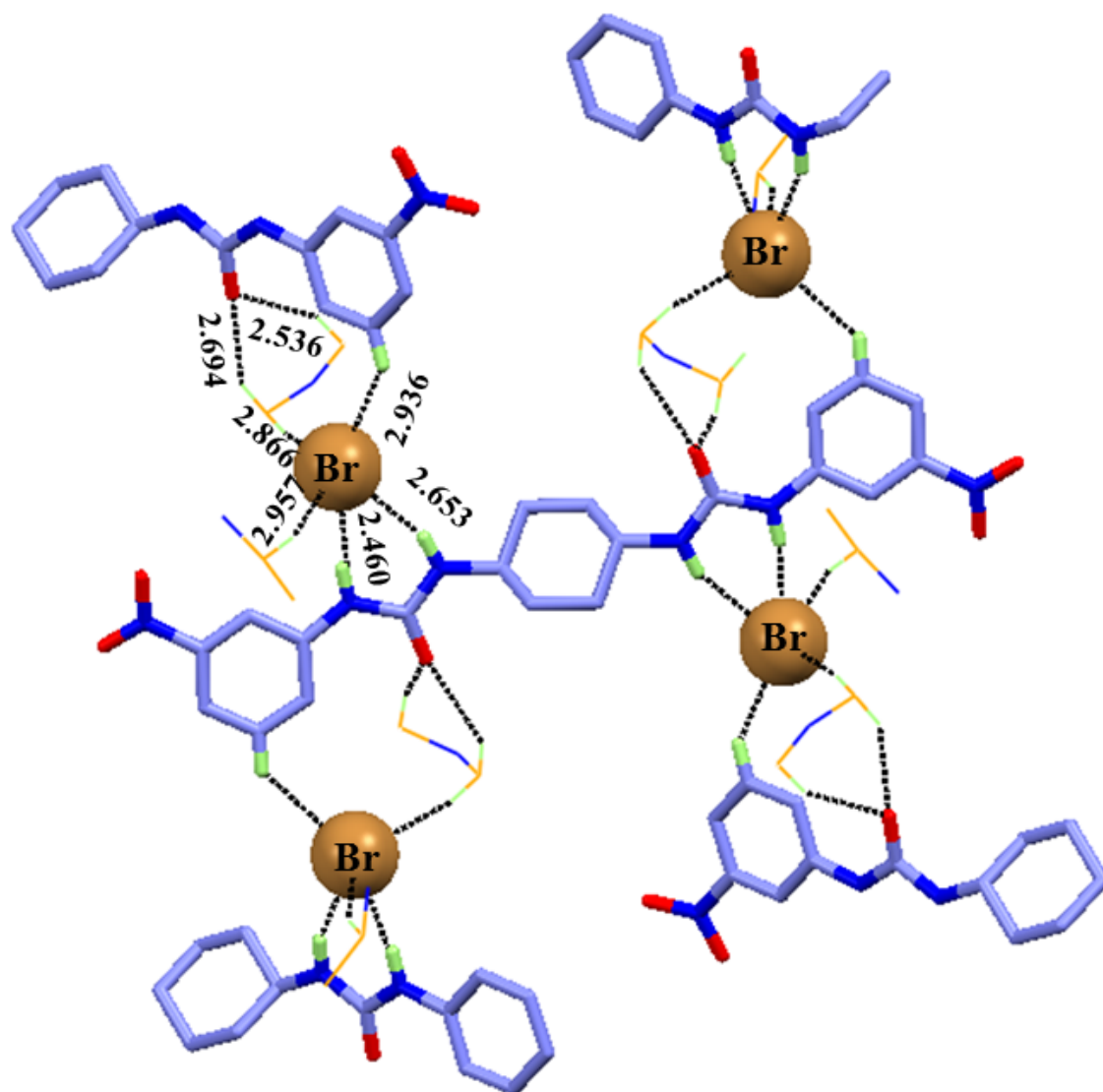


**Figure S20:** X-ray structure analysis of complex **1b** showing coordination environment of anion as well as extra stabilization through two C-H<sub>aliphatic</sub>...O<sub>urea</sub> with proper bond distances in Angstrom.

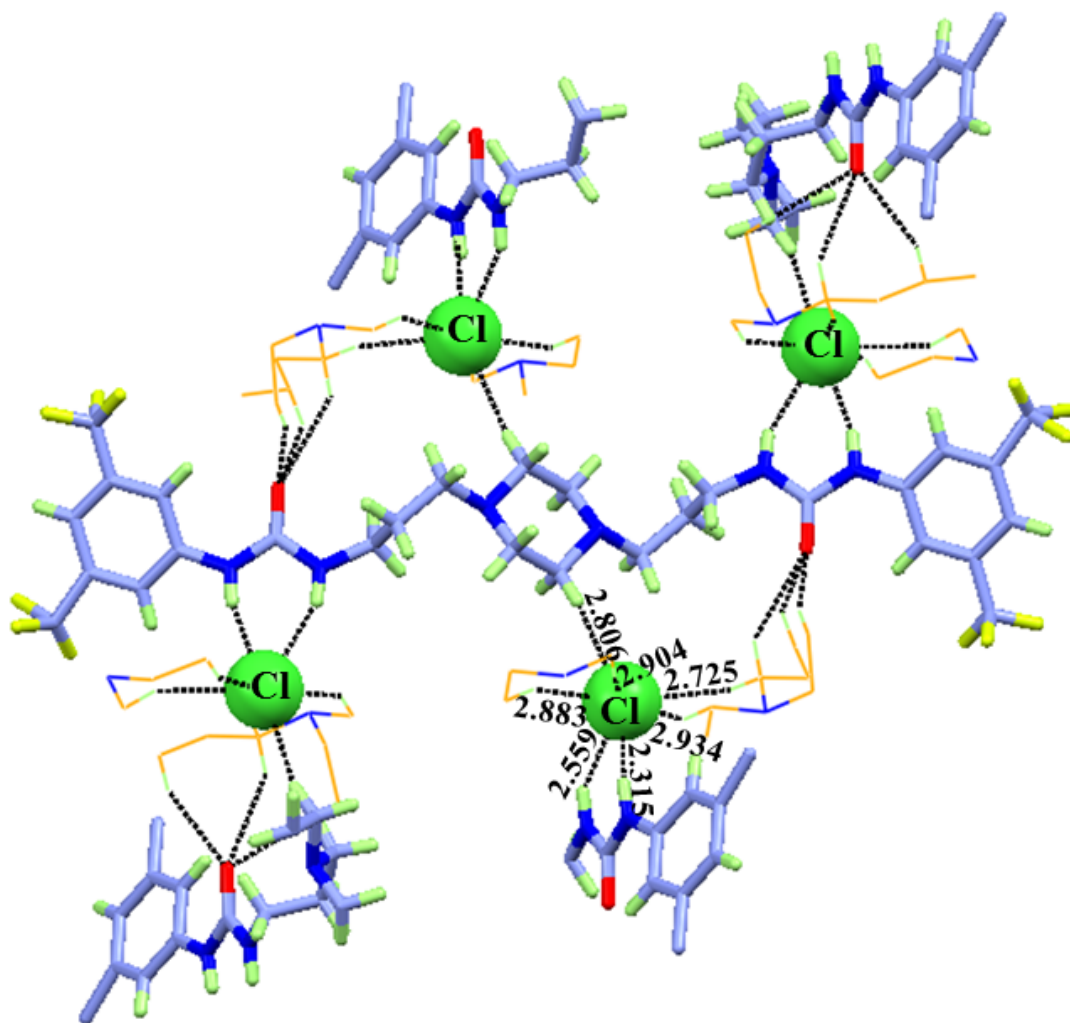


**Figure S21:** X-ray structure analysis of complex **2a** showing coordination environment of anion as well as extra stabilization through two C-H<sub>aliphatic</sub>...O<sub>urea</sub> with proper bond distances in Angstrom.

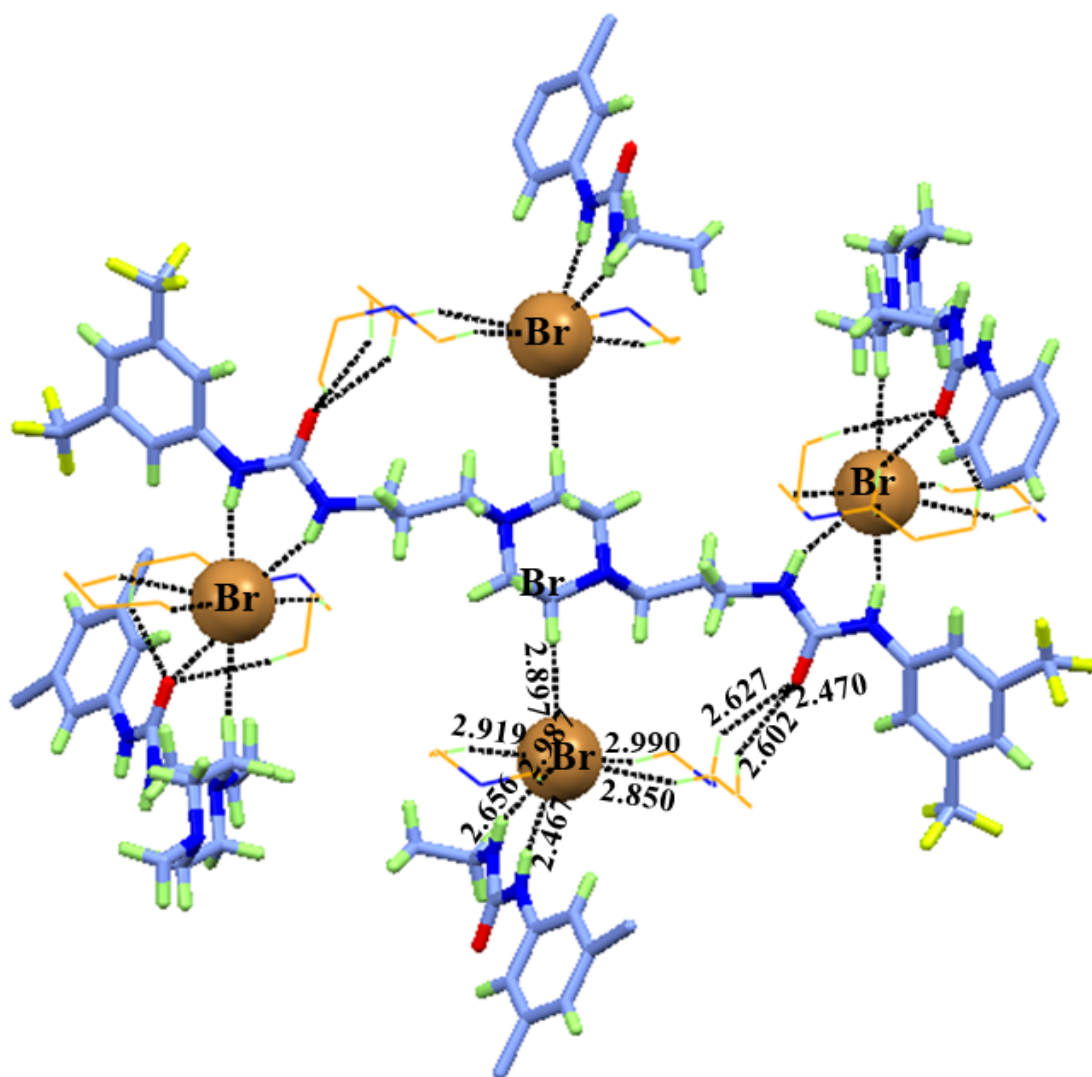


**Figure S22:** X-ray structure analysis of complex **2b** showing coordination environment of anion as well as extra stabilization through two C-H<sub>aliphatic</sub>...O<sub>urea</sub> with proper bond distances in Angstrom.

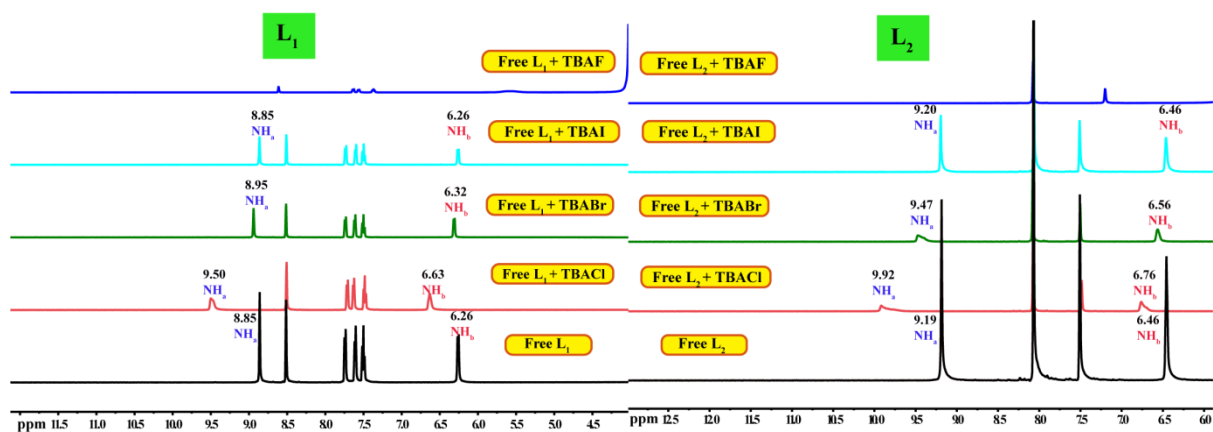
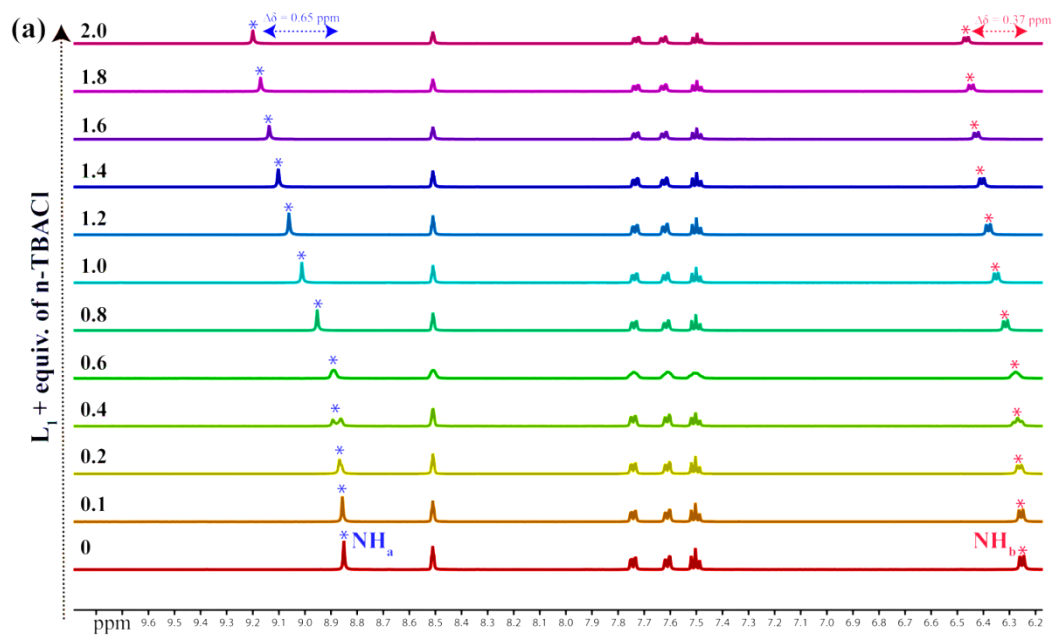


**Figure S23:** Partial <sup>1</sup>H NMR spectra (600 MHz, DMSO-d<sub>6</sub>) of L<sub>1</sub> and L<sub>2</sub> and the maximum observable shifts in urea-NH protons upon the addition of excess Cl<sup>-</sup>, Br<sup>-</sup>, I<sup>-</sup>, F<sup>-</sup> in the form of their TEA/n-TBA salts.

### Anion binding analysis by <sup>1</sup>H-NMR titrations

The <sup>1</sup>H NMR titration of L<sub>1</sub> and L<sub>2</sub> was performed in DMSO-d<sub>6</sub> solvent. The stock solutions of the compound (L<sub>1</sub> and L<sub>2</sub> ; 10 mM), tetrabutyl ammonium Chloride (TBACl; 2 M) and tetrabutyl ammonium Bromide (TBABr; 2 M) were prepared in DMSO-d<sub>6</sub>. The TBACl and TBABr were used as the source of Cl<sup>-</sup> and Br<sup>-</sup> ion. The changes in chemical shift ( $\Delta\delta$ ) value of the N-H protons of the urea-moieties were analysed. Significant extents of chemical shift ( $\Delta\delta$ ) of both N-H protons were observed during titration with chloride solution. All <sup>1</sup>H NMR spectra were stacked through the MestReNova software. Changes in chemical shift against the concentration of Cl<sup>-</sup> ion were fitted using BindFit v 0.5 program.<sup>1</sup>



(b)

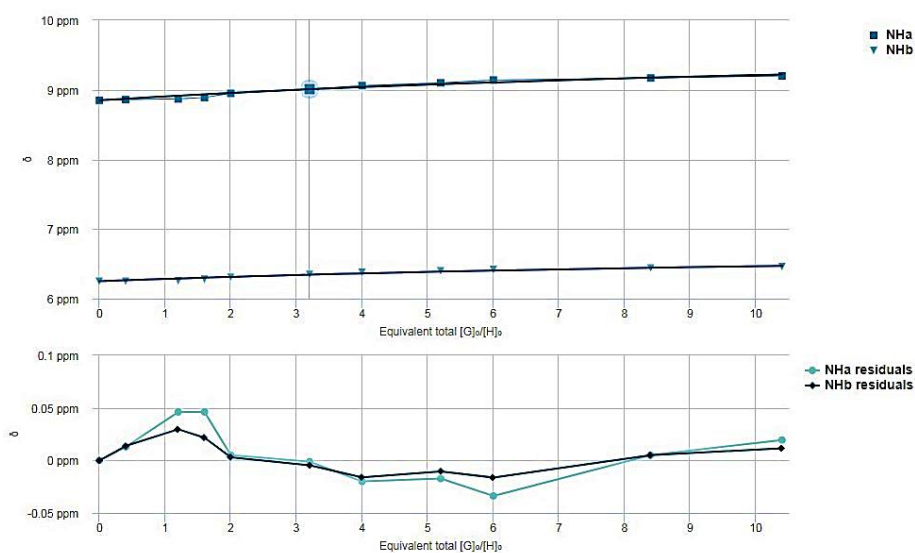


**Figure S24:** (a) Expanded partial  $^1\text{H}$  NMR spectra of  $\text{L}_1$  upon titration with n-TBACl in  $\text{DMSO-d}_6$ . (b) Showing the raw vs. fitted data (fitted to 1:1 NMR binding data) (top) and the corresponding residual plot (bottom). Binding constant ( $K$ ) =  $4.50 \text{ M}^{-1}$  (Ref. 2).

(<http://app.supramolecular.org/bindfit/view/4fc6d6b1-2de2-43c5-af72-bbd18e997501>)

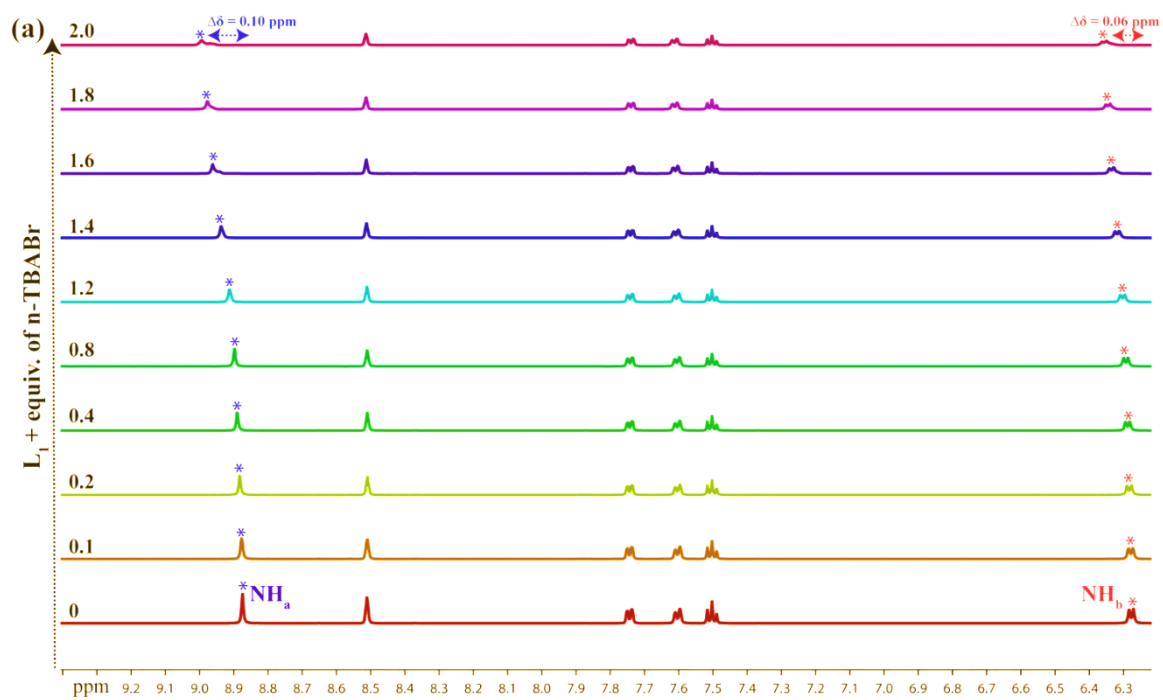
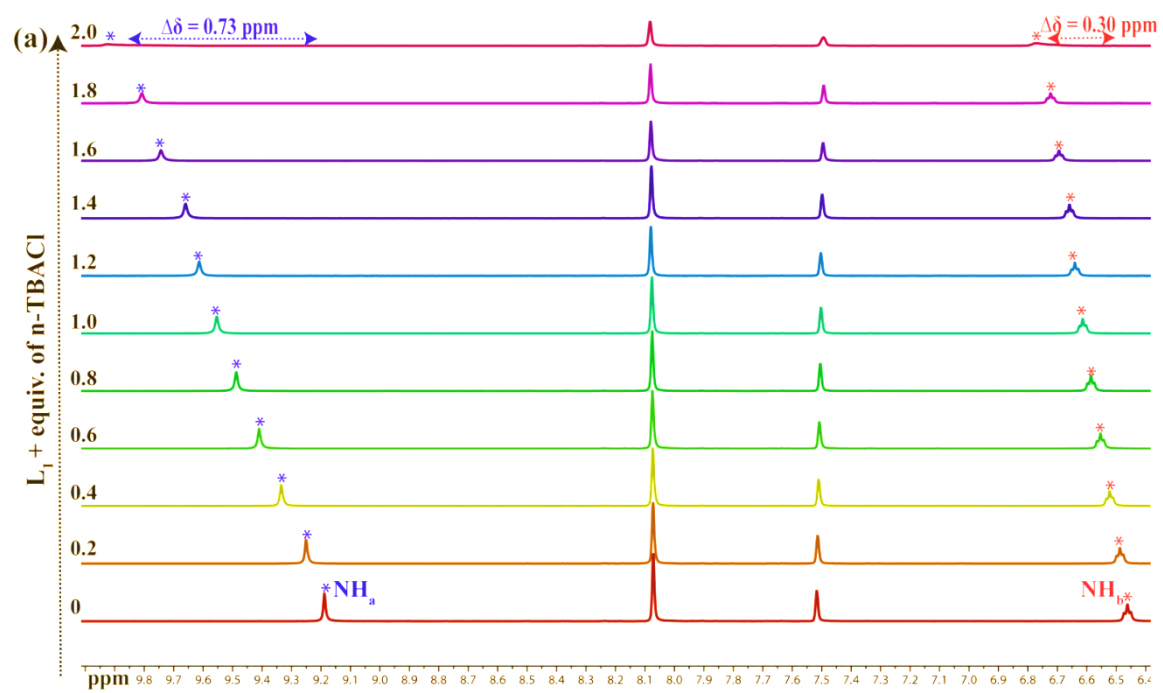


**Figure S25:** (a) Expanded partial  $^1\text{H}$  NMR spectra of  $\text{L}_1$  upon titration with n-TBABr in  $\text{DMSO-d}_6$ .



(b)

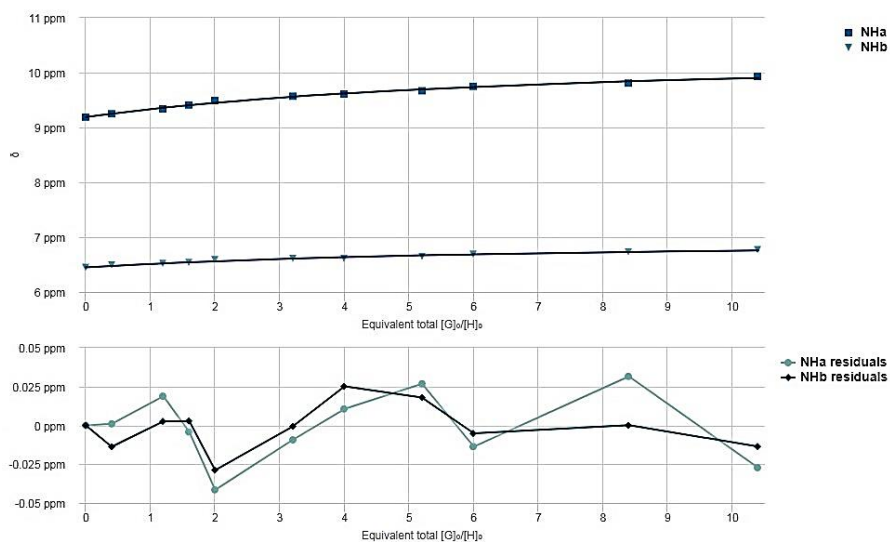


**Figure S26:** (a) Expanded partial  $^1\text{H}$  NMR spectra of  $\text{L}_2$  upon titration with n-TBACl in  $\text{DMSO-d}_6$ . (b) Showing the raw vs. fitted data (fitted to 1:1 NMR binding data) (top) and the corresponding residual plot (bottom). Binding constant ( $K$ ) =  $12.96 \text{ M}^{-1}$  (Ref. 2).

(<http://app.supramolecular.org/bindfit/view/df8b0a98-517a-4b88-88d5-cd99e39c582d>)

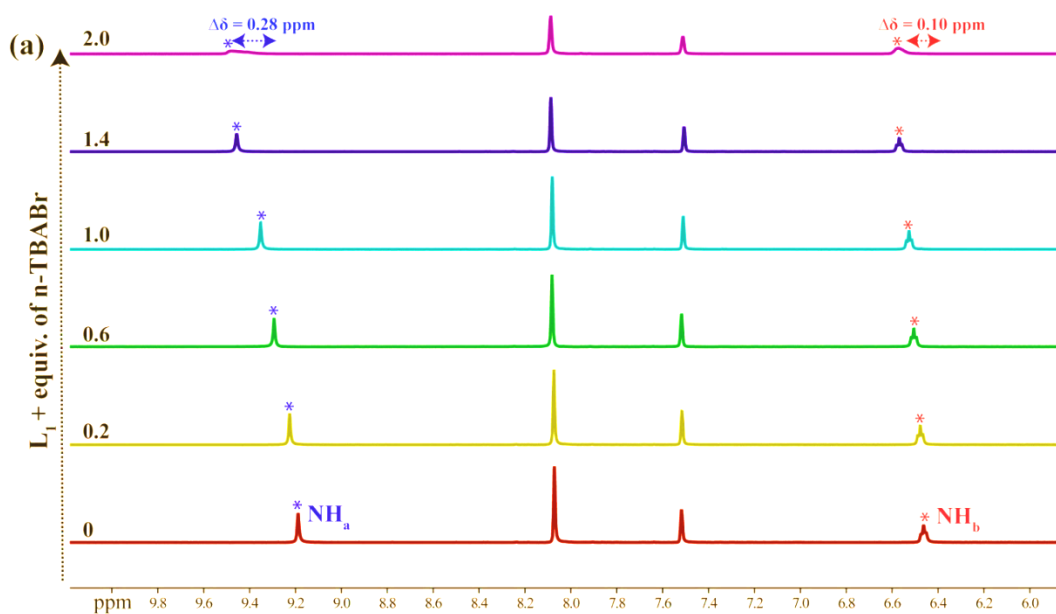


**Figure S27:** (a) Expanded partial  $^1\text{H}$  NMR spectra of  $\text{L}_2$  upon titration with n-TBABr in  $\text{DMSO-d}_6$ .

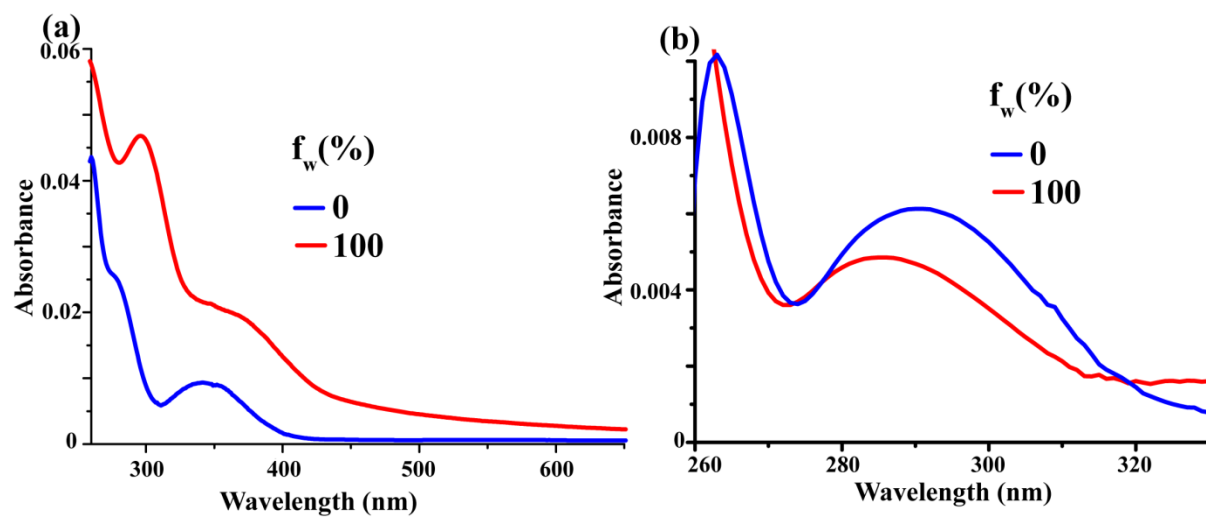


**Figure S28:** (a) UV-Vis changes of  $L_1$  (2  $\mu\text{M}$ ) (b)  $L_2$  (2  $\mu\text{M}$ ) in several solvents at room temperature.

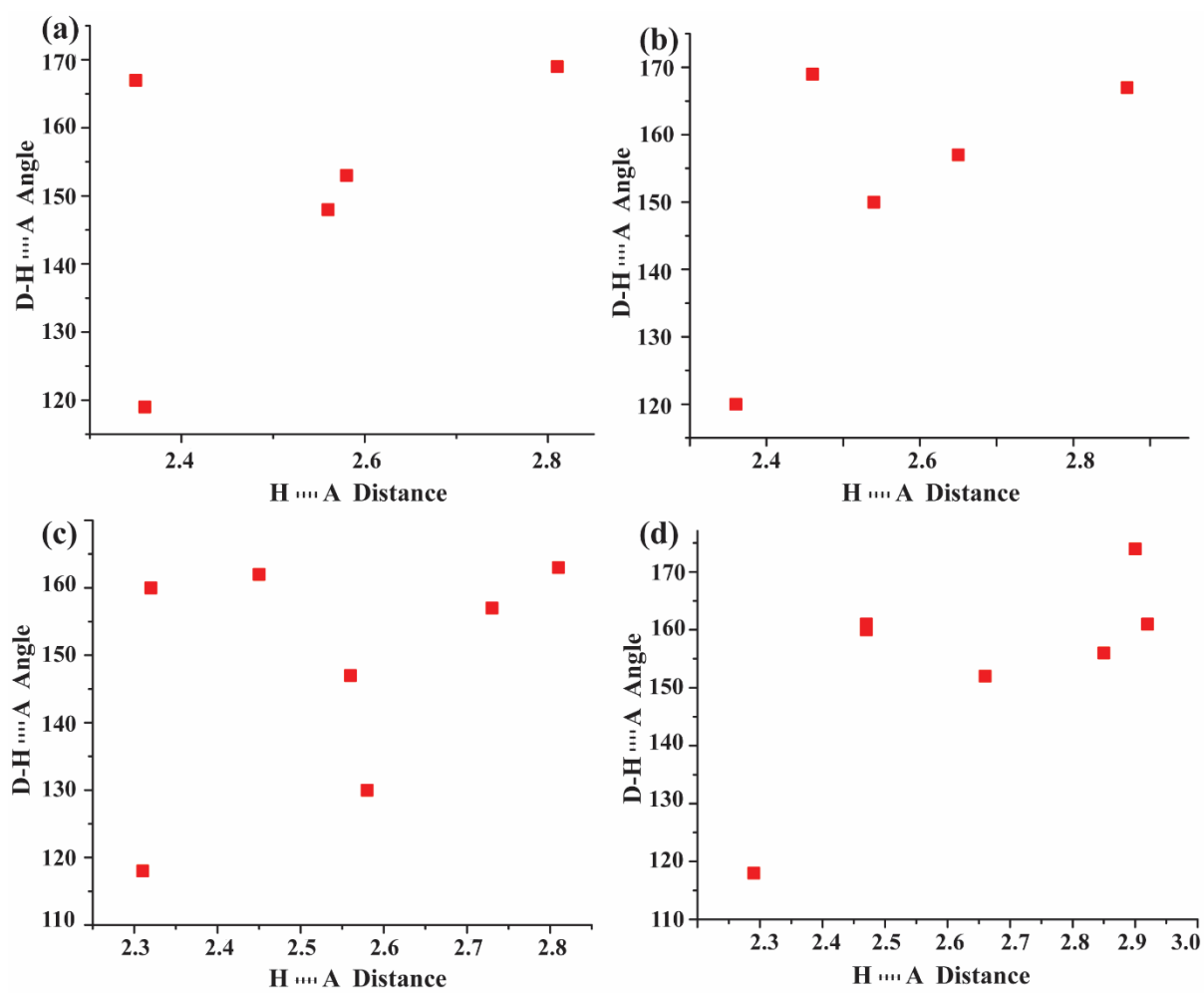


**Figure S29:** The scatter plot of N-H...A angle vs. H...A distance of the hydrogen bonds in the complexes (**1a**, **1b**, **2a**, **2b**).

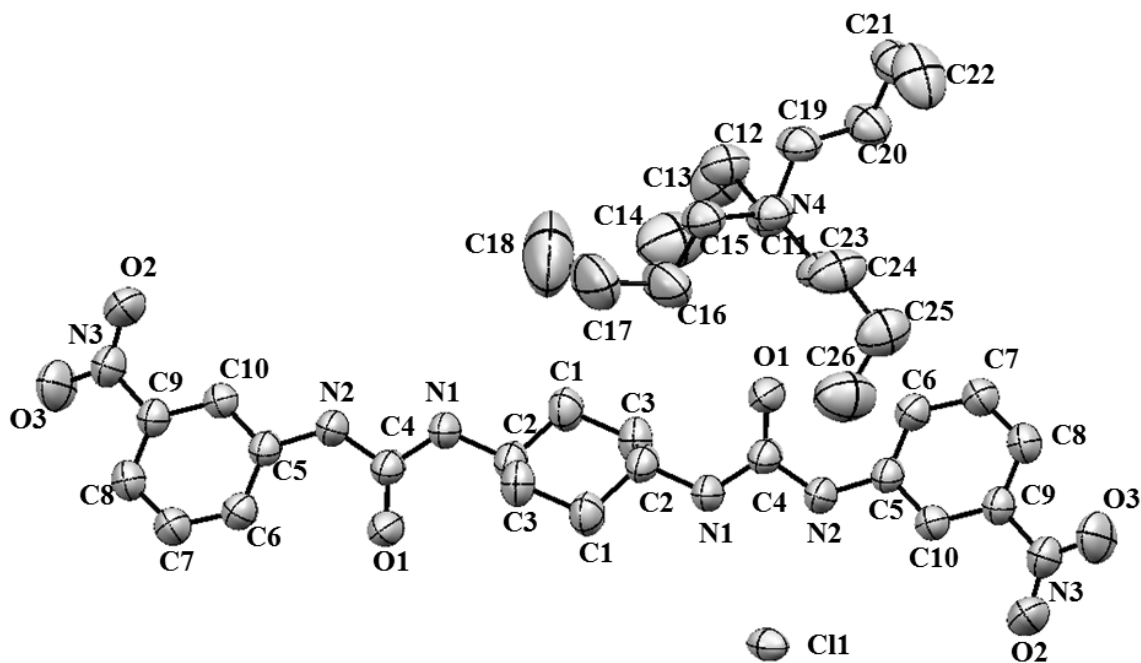


Figure S30: ORTEP diagram of 1a.

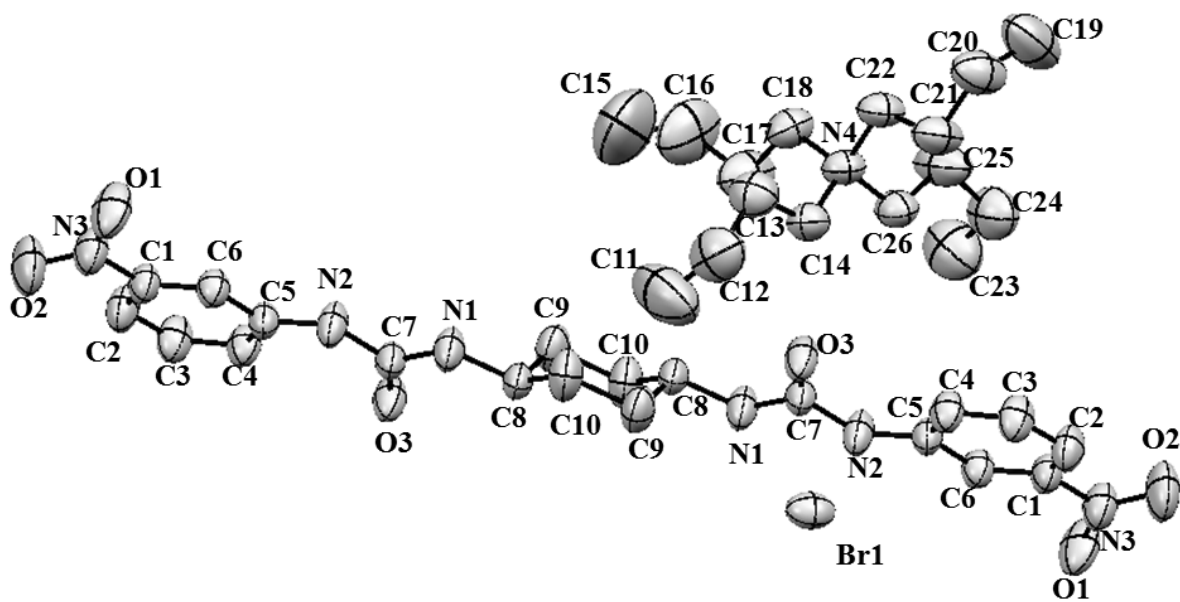


Figure S31: ORTEP diagram of 1b.

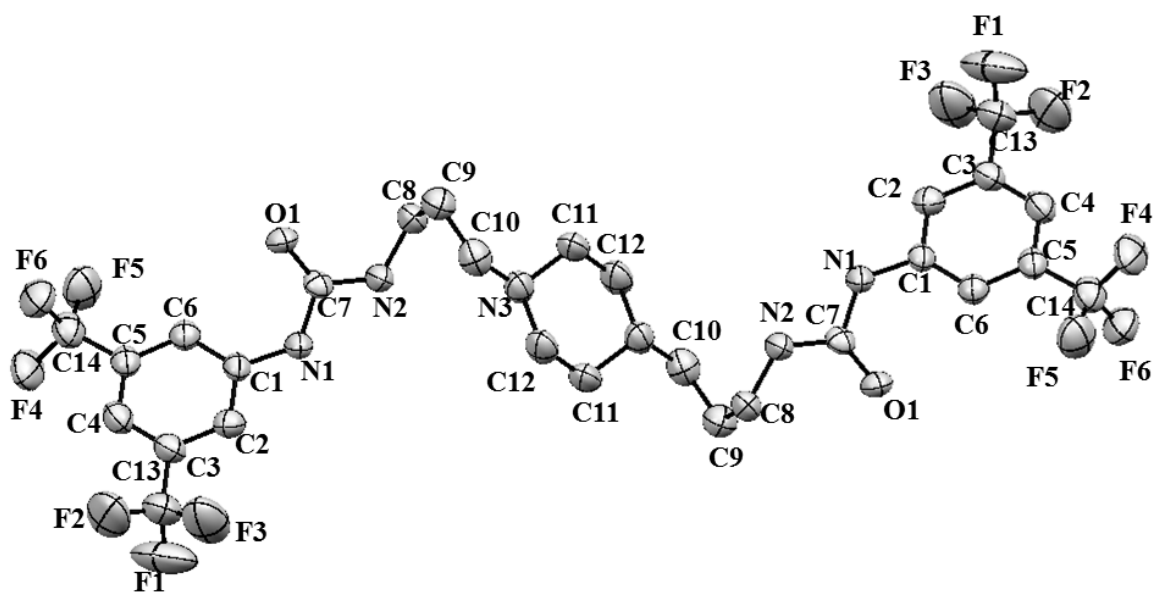


Figure S32: ORTEP diagram of L<sub>2</sub>.

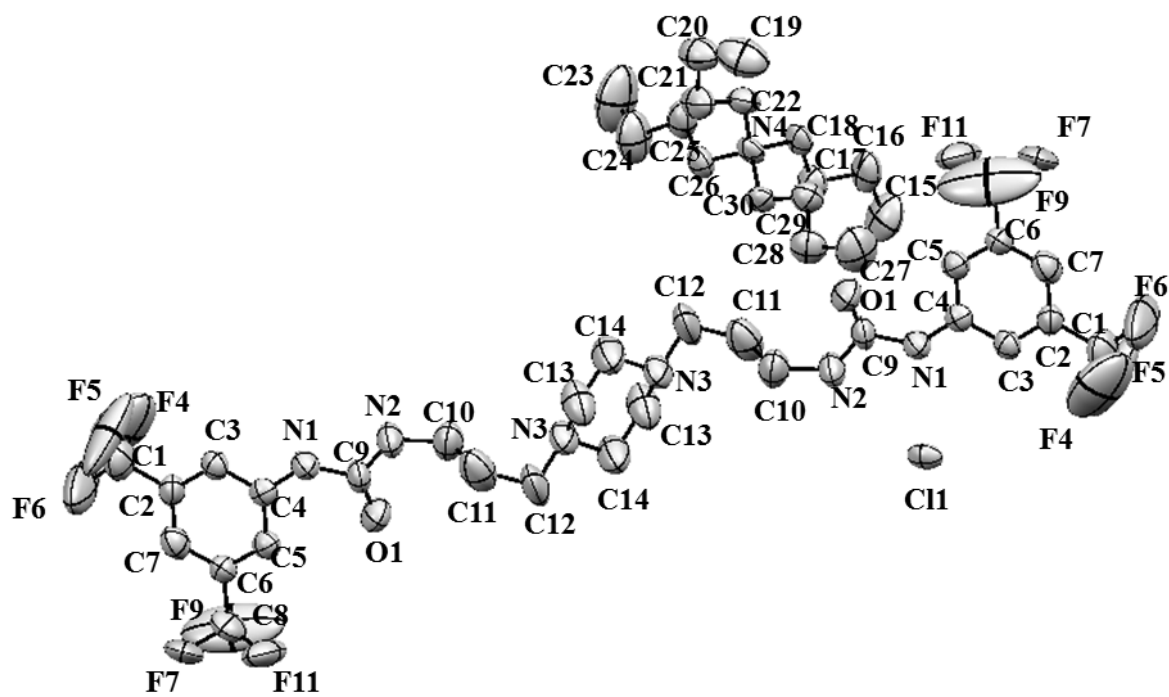


Figure S33: ORTEP diagram of 2a.

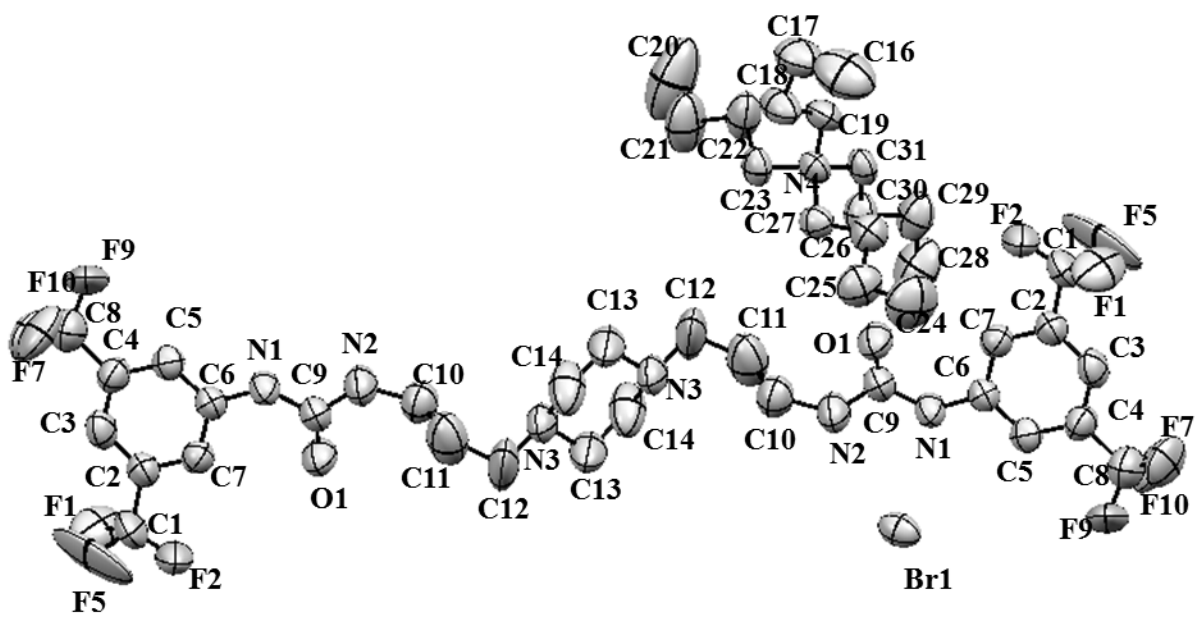
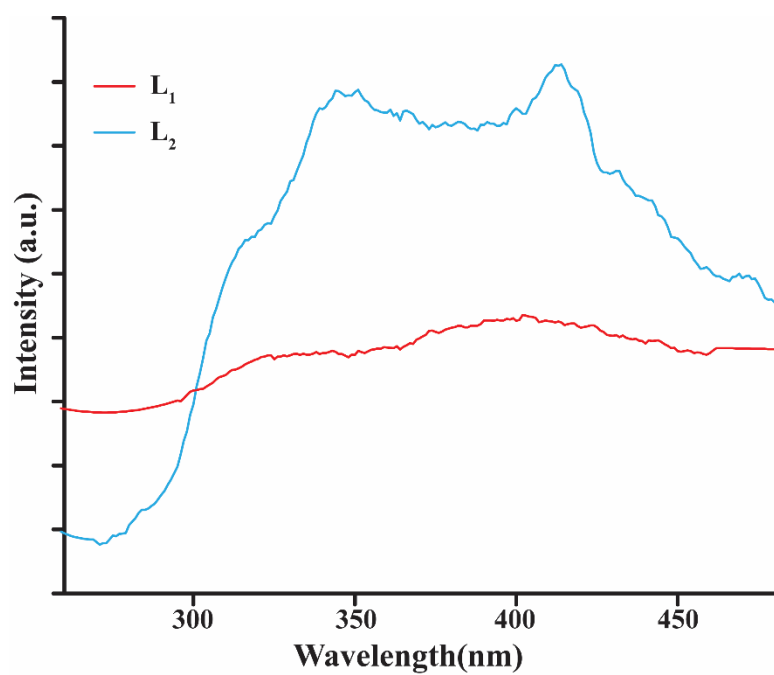


Figure S34: ORTEP diagram of 2b.



**Figure S35:** Solid state fluorescence spectra of L<sub>1</sub> and L<sub>2</sub>.

**References:**

1. D. Brynn Hibbert and P. Thordarson, Chem Commun, 2016, 52, 12792-12805.
2. <http://supramolecular.org>

**Table S1:** Hydrogen bonding distances (Å) and Bond angles (°) in the neutral anion-receptor complexes:

Complex	D–H···A	d(D···H)/Å	d(H···A)/Å	d(D···A)/Å	<D–H···A/°	Symmetry codes
1a	N1-H1N···C11	0.86	2.58	3.367(4)	153	x,1/2-y,1/2+z
	N2-H2N···C11	0.86	2.35	3.192(4)	167	x,1/2-y,1/2+z
	C6-H6···O1	0.93	2.36	2.930(5)	119	x, y, z
	C11-H11A ··· C11	0.97	2.81	3.763(5)	169	x, y, z
	C23-H23A··· O1	0.97	2.56	3.426(5)	148	x, y, z
1b	N1-H1···Br01	0.86	2.65	3.459(3)	157	x,1/2-y,-1/2+z
	N2-H2A···Br01	0.86	2.46	3.309(2)	169	x,1/2-y,-1/2+z
	C4-H4···O3	0.93	2.36	2.935(4)	120	x,y,z
	C14-H14B···Br01	0.97	2.87	3.816(3)	167	x,y,z
	C26-H26A···O3	0.97	2.54	3.412(4)	150	x,y,z
2a	N1-H1N···C11	0.86	2.32	3.136(6)	160	x,y,z
	N2-H 2N···C11	0.86	2.56	3.315(6)	147	x,y,z
	C5-H5···O1	0.93	2.31	2.865(8)	118	x,y,z
	C14-H 14A··· C11	0.97	2.81	3.745(8)	163	x,1/2-y,-1/2+z
	C17-H17B···O1	0.97	2.45	3.388(7)	162	x,1/2-y,1/2+z
	C28-H28B··· O1	0.97	2.58	3.286(8)	130	x,1/2-y,1/2+z
	C30-H 30A··· C11	0.97	2.73	3.637(6)	157	x,y,z
2b	N1-H1···Br1	0.86	2.47	3.292(6)	161	x,y,z
	N2-H2···Br1	0.86	2.66	3.439(8)	152	x,y,z

	C7-H7...O1	0.93	2.29	2.850(11)	118	x,y,z
	C13-H13B... Br1	0.97	2.90	3.863(10)	174	x,1/2-y,-1/2+z
	C22-H22A... Br1	0.97	2.92	3.850(10)	161	x,1+y,z
	C27-H27A... Br1	0.97	2.85	3.755(8)	156	x,y,z
	C30-H30B...O1	0.97	2.47	3.399(10)	160	x,1/2-y,1/2+z
2	N1-H1N... O1	0.86	2.06	2.893(5)	162	x,1/2-y,1/2+z
	N2-H2N... O1	0.86	2.26	3.035(6)	149	x,1/2-y,1/2+z
	N3-H3N...N2	0.98	2.57	3.205(6)	123	x,y,z
	C6-H6...O1	0.93	2.47	2.933(6)	111	x,y,z

**Table S2:** Contact contributions from the  $d_{\text{norm}}$  surface areas of dipodal segments in free receptors and in anion complexes.

<b>Bond</b>	<b>1a</b>	<b>1b</b>	<b>2a</b>	<b>2b</b>	<b>L<sub>2</sub></b>
C...H/H...C	3.3/2.4	3.4/2.5	3.0/2.8	4.4/3.0	2.5/2.0
O...H/ H...O	7.0/6.1	7.2/6.3	0.2/0.2	0.2/0.2	3.7/3.3
F...H	0	0	9.4	9.5	15.6
N...H	1.1	1.1	1.0	0.9	1.0
H...H	65.4	63.4	55.3	53.6	31.0
Cl...H	5.0	0	3.5	0	0
Br...H	0	5.1	0	4.0	0